Materials Letters 134 (2014) 16–19

Contents lists available at ScienceDirect

Materials Letters

journal homepage: www.elsevier.com/locate/matlet

Enhanced performance of dye-sensitized solar cells using silica/gold core–shell spheres modified photoanodes

Qingsong Jiang [a,b], Jian Gao [b], Hong Tao [c], Guojia Fang [c], Helin Wei [b,*], Lin Yi [b,*]

[a] *Faculty of Mathematics and Physics, Huaiyin Institute of Technology, Huai'an 223003, PR China*
[b] *School of Physics, Huazhong University of Science and Technology, Wuhan 430074, PR China*
[c] *School of Physics and Technology, Wuhan University, Wuhan 430072, PR China*

ARTICLE INFO

Article history:
Received 27 March 2014
Accepted 2 July 2014
Available online 9 July 2014

Keywords:
Nanoparticles
Optoelectronic materials
Sol–gel preparation

ABSTRACT

This paper describes a series of dye-sensitized solar cells (DSSCs) including TiO_2 photoanodes with different amounts of silica/gold core–shell (SiO_2@Au) spheres. The results show that the DSSC containing TiO_2 photoanode with a certain amount of SiO_2@Au spheres can attain its relatively better power conversion efficiency of 5.29%. Compared with a reference DSSC containing a pure TiO_2 photoanode, the power conversion efficiency of the DSSC has been remarkably enhanced by 33.9%.

1. Introduction

Dye-sensitized solar cells (DSSCs) have attracted a tremendous attention because of their low-cost, simple fabrication process, and higher up scaling [1]. Recently, there are several methods to enhance the power conversion efficiency (η) of DSSCs by increasing the light harvesting efficiency of photoanodes. The enhancement of dye loading is one of the effective methods [2]. The enhancement of light path is also one of the effective methods by light-scattering [3].

Noble metal nanoparticles (such as Ag and Au) have been found to be another effective method because of the localized surface plasmon resonance (LSPR). Light-scattering probably also plays important factor while LSPR exists. Many efforts had been made to investigate the effect of noble metal nanoparticles on the performance of DSSCs [4,5]. Different structures such as Au@TiO_2 hollow spheres and Au@SiO_2 spheres were also incorporated in TiO_2 films, respectively [6,7]. The results showed that the η of the DSSCs was increased significantly because of the LSPR. The η of DSSCs based on the photoanode containing TiO_2@Au@TiO_2 spheres increased from 8.3% to 10.8% because of plasmon enhanced photoabsorption in the long-wavelength region of solar spectrum [8]. Herein, SiO_2@Au spheres are designed and synthesized. The composite TiO_2 films are also fabricated by adding a small amount of SiO_2@Au spheres. The effect of different amounts of SiO_2@Au spheres on the performance of DSSCs is systematically investigated.

2. Experimental methods

SiO_2@Au spheres were synthesized and dispersed into deionized water with the silica concentration of 6 mg/ml [9]. The composite TiO_2 pastes were fabricated according to a reported process by Gratzel [10]. The composite TiO_2 films were coated on FTO by a doctor-blade method, and sensitized by immersing them in 0.5 mM ethanol solution of N719 for 12 h at 60 °C. The photoanodes were obtained by washing the composite TiO_2 films with ethanol and drying for the test [11]. A platinized FTO counter electrode was fabricated by a radio frequency magnetron sputtering system. The typical DSSCs were assembled in a sandwich structure by an open cell. The photoactive area of DSSCs was 0.2 cm^2. The detailed experimental procedures are described in Supporting information.

3. Results and discussion

Characterization of SiO_2@Au spheres: The monodisperse silica spheres with 215 ± 9 nm in diameter are fabricated by the modified Stober method as shown in Fig. 1(a). SiO_2@Au-seed spheres are obtained by the electrostatic effect [9]. After the growth of Au-seed, the SiO_2@Au spheres are synthesized as shown in Fig. 1(b). The mean diameter of SiO_2@Au spheres is 250 ± 9 nm. The thickness of Au nanoshells is about 18 nm. The result agrees well with the previous reports [9]. Lattice fringe image corresponding to Au nanoshells is shown in the inset of Fig. 1(b). The observed interplanar distance of 0.236 nm agrees well with the (111) plane spacing of Au [12].

---

* Corresponding authors.
E-mail addresses: hlwei@mail.hust.edu.cn (H. Wei), yilin@mail.hust.edu.cn (L. Yi).

http://dx.doi.org/10.1016/j.matlet.2014.07.007
0167-577X/

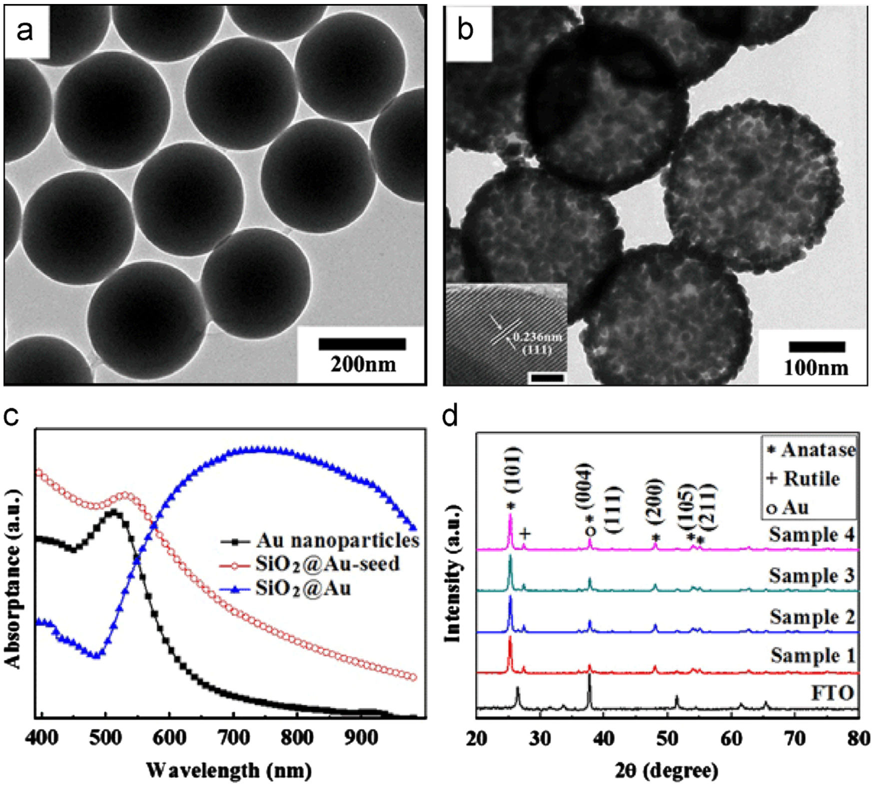

Fig. 1. TEM images of (a) silica spheres and (b) SiO_2@Au spheres. (c) Normalized absorption spectra of the Au nanoparticles, SiO_2@Au-seed spheres, and SiO_2@Au spheres in aqueous solution. (d) XRD patterns of the composite TiO_2 films. The inset of (b) is the HRTEM image of SiO_2@Au spheres. The scale bar of the inseted figure is 2 nm.

The normalized absorption spectra of the Au nanoparticles, SiO_2@Au-seed spheres, and SiO_2@Au spheres are shown in Fig. 1(c). The absorption peak wavelength of Au nanoparticles is around 512 nm due to the LSPR of Au nanoparticles. The absorption peak appears at about 532 nm for SiO_2@Au-seed spheres due to the high refractive index of the surrounding environment of Au nanoparticles. The absorption wavelength of SiO_2@Au spheres is around 739 nm. The redshift of the absorption peak can be attributed to the enhancement of the interparticle plasmon coupling and the LSPR of the Au nanoparticles [9].

Characterization of composite TiO_2 film: The SiO_2@Au spheres are used as additives to modify the TiO_2 films with different mass fractions (SiO_2 of SiO_2@Au spheres: P25=0%, 0.01%, 0.05%, and 0.1%), which are defined as sample 1, 2, 3, and 4. The X-Ray Diffraction (XRD) patterns of FTO and four samples are shown in Fig. 1(d). The five characteristic peaks of anatase are observed, and there is a weak characteristic peak of rutile in all films. It is obvious that the (004) diffraction intensity for anatase in sample 2, 3, and 4 is larger than that in sample 1 due to overlapping the (004) diffraction peak of anatase with the (111) diffraction peak of Au. The cross-sectional scanning electron microscope (SEM) images of the composite TiO_2 films are shown in Fig. 2(a–d). It is obvious that the thicknesses of sample 1, 2, 3, and 4 are 12.3 μm, 12.9 μm, 12.2 μm, and 12.8 μm, respectively. Therefore, the different amounts of dye adsorbed, which results from the different film thicknesses, can be neglected. The plane-view SEM images of the composite TiO_2 films are also shown in the insets of Fig. 2(a–d). The composite TiO_2 films exhibit compact structure and smooth surface.

Photoelectric performance of DSSCs: The photocurrent density–voltage (J–V) curves of the DSSCs are shown in Fig. 3(a). The photovoltaic parameters of all the DSSCs are summarized in Table 1. The results show that the fill factor (FF) remains almost unchanged. It is obvious that open-circuit voltage (V_{oc}) and short-circuit current density (J_{sc}) increase with increasing the amount of the SiO_2@Au spheres with silica mass fraction ranging from 0% to 0.05%. The DSSC based on sample 3 shows the maximum V_{oc} of 0.68 V and J_{sc} of 11.45 mA cm^{-2}. The η of the DSSC also reaches its maximum value of 5.29%, and 33.9% higher than that of the DSSC based on sample 1 (3.95%). The enhancement of the V_{oc} from 0.65 V to 0.68 V is because the quasi-Fermi level in the composite TiO_2 films shifts to more negative level which results from the electron storage effects of the Au nanoshells [12–14]. There are two reasons to explain the increase of the J_{sc}. On one hand, Au nanoshells enhance the light absorption of dye molecules because of the LSPR of SiO_2@Au spheres. On the other hand, the SiO_2@Au spheres are also used as light scattering centers to enhance the light path. However, J_{sc} decreases with increasing the excess SiO_2@Au spheres (silica mass fraction more than 0.05%) probably because of the lower dye absorption [12]. The Au nanoshells are also taken as recombination sites. The excess SiO_2@Au spheres can generate the bigger recombination probability. Thus, the V_{oc} is also decreases a little [5].

The electrochemical impedance spectroscopy (EIS) is also shown in Fig. 3(b). The Nyquist plots of the four-sample show two semicircles. The main point of our study is to illustrate the mechanism of the charge transport and recombination at the TiO_2/dye/electrolyte interface. The semicircle at low frequency represents the electron transport resistance (R_t) and the interfacial charge recombination resistance (R_{ct}) paralleled with the interfacial capacitance at the TiO_2/dye/electrolyte interface. Under one sun illumination intensity, the R_t can be negligible by applying bias voltage of the V_{OC} [15,16]. The larger R_{ct} value demonstrates the less charge recombination probability between the injected electrons in TiO_2 and I_3^- ions in the liquid electrolyte. From Fig. 3(b) and Table 1, the R_{ct} values of DSSCs increase with increasing the amount of the SiO_2@Au spheres. These results imply that the SiO_2@Au spheres are in favor of injecting charge into TiO_2 film, due to the LSPR of SiO_2@Au spheres. However, the R_{ct} value of the DSSC